



Green Synthesis of Silver Nanoparticles using *Tragopogon Collinus* Leaf Extract and Study of Their Antibacterial Effects

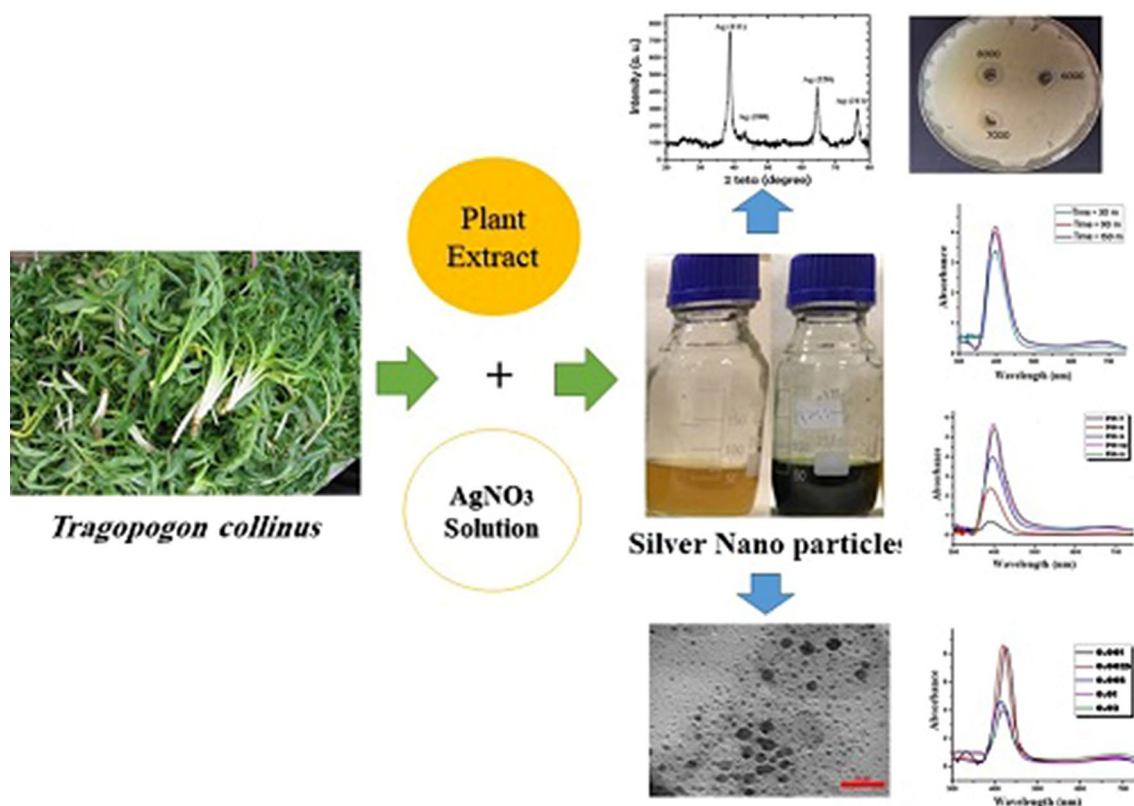
Roya Seifipour¹ · Maryam Nozari² · Leila Pishkar¹

Received: 29 November 2019 / Accepted: 6 January 2020 / Published online: 11 January 2020
© Springer Science+Business Media, LLC, part of Springer Nature 2020

Abstract

In this research, “*Tragopogon collinus*” extract was used for synthesis of silver nanoparticles and their biological properties were studied. Based on this, the extract of the plant was prepared and the synthesis of silver nanoparticles under different conditions were investigated. The best conditions for the synthesis of nanoparticles were 0.0025 M of silver nitrate, temperature of 40 °C, pH 10 and 20 cc of the extract, which the formation of the nano particles were confirmed by UV–Vis, TEM, XRD, FT-IR analysis. Average size of the particles were obtained 7 nm and the formation of the nano silver crystals was proved. The synthesized silver nanoparticles showed inhibition zone for both Gram-positive and -negative bacteria and *Staphylococcus aureus* has better result compared to *Escherichia coli*.

Graphic Abstract



Extended author information available on the last page of the article

Keywords *Tragopogon collinus* leaf extract · Silver nano particles · Green synthesis · UV–Vis spectroscopy · Anti-bacterial effects

1 Introduction

Nanoparticles are a special group of materials with unique properties [1–4]. Nanoscale metal particles are among the important nanotechnology products. These particles have attracted interest due to their unique optical properties, catalytic nature and electromagnetic applications [5]. Although various chemical and physical methods are commonly used for production of nanoparticles, they come with disadvantages such as use of hazardous chemicals, production of wastes that pollute the environment, high energy consumption and low efficiency. Hence, scientists are looking for new methods for production of nanoparticles, among which biosynthesis of nanoparticles has attracted great interest due to its compatibility with the environment and its economic advantages [6, 7]. Plants, algae, fungi, yeast, bacteria and viruses can be used in biosynthesis of nanoparticles [3, 5, 8–11]. Numerous natural plants and plant products are available that can be easily used to facilitate biosynthesis of nanoparticles, because they have the compounds include alkaloids, tannins, steroids, phenols, saponins and flavonoids in their structure which can help in reduction of silver ions to silver nanoparticles by various functional groups such as hydroxyl, ketone and aldehydes [10, 12, 13]. Silver nanoparticles have many research applications in medical engineering, pharmacy, etc. [3, 14]. Chemical nanoparticles cause environmental hazards and toxicity and, of course, are costly. However, biological nanoparticles are not hazardous to the environment given that they are produced from plants [6]. Moreover, increasing antibiotic resistance raises treatment costs, increases recovery period and leads to antibiotic treatment failure. Therefore, it is necessary to manufacture new antibiotic agents, use more novel and comprehensive treatment methods to control infections and prevent the spread of antibiotic-resistant pathogens [15, 16]. Moreover, occurrence of dangerous and fatal complications such as anaphylactic shock and liver and kidney failure in some patients necessitates the use of new antibacterial materials. Application of nanoparticles in medicine as antibacterial materials is expanding with the advancement of nanoscience, easier production of silver nanoparticles, and proof of their antimicrobial properties [15, 16]. Silver nanoparticles have been developed as an antibacterial, antiviral and anti-decay agent [17, 18]. These particles act as an effective lethal agent against a wide range of Gram-positive and Gram-negative bacteria and even against antibiotic-resistant strains [19, 20].

So many articles have been published on producing silver nano particles using green method and plant extract. Some of them are: banana peel [21], *Azadirachta indica*

leaf extract [14], *Neem* leaves [22], *Carob* leaf [23], *Olive* leaf [24], *Ocimum tenuiflorum* leaf extract [25], *Salanum tricobatum* [25], *Urtica dioica* Linn.[26], *Datura Stramonium* [27], *Combretum erythrophyllum* [28], *Shikakai* [29], *Sida cordifolia* [30], *Zataria multiflora* [31], *Megaphrynium macrostachyum* [32], *Embelia ribes* [33], *Enico stemma axillare* [34], Green tea (*Camellia sinensis*) [35], *Azadirachta indica* leaf extract [36], *Ocimum Sanctum* leaf extract [36], green Coffee bean [37], Coffee extract [38], *Givotia moluccana* [9].

Tragopogon collinus is a wild plant of the *Asteraceae* family and one of the edible native plants in Iran. This plant is a stomach tonic and topical application of its root is effective in treating severe poisoning, infections and ear drainage. So, attending to the benefits, in this research silver nano particles was produce from *T. collinus* extract. Different conditions (Time of the reaction, quantity of extract, temperature, pH of the solution and concentration of silver nitrate solution) were investigated and the produced nano particles were characterized by UV–Vis spectrophotometry, FT-IR, XRD and TEM analyses. Furthermore the achieved silver nano particles was tested for antibacterial activities as well.

2 Experimental Section

2.1 Materials

AgNO₃ (100%), Ethanol (99%), Methanol (99%), HCl (37%), NH₃ (25%), Na₂CO₃ (99.9%), Muller-Hinton-Agar and Muller-Hinton-Broth were from Merck chemical company, Folin–Ciocalteu reagent and Gallic Acid was from Sigma-Aldrich Company.

2.2 Instrumentation

The UV–Vis spectra was recorded using 530 Jasco (Japan) spectrophotometer, XRD patterns was performed using X-Ray analyzer model SCIFERT-3003 PTS, the FT-IR spectra was obtained by Thermo Nicolet Nexus 870 FT-IR spectrometer and the surface morphology of the synthesized nano particles has been studied using Transmission electron microscopy (Model: JSM 2010).

2.3 Preparation of the Plant Extract

Tragopogon collinus plants were bought in spring from the local market in Iran and washed and dried in the dark and kept in a cool place away from sunlight. Two solvents

(ethanol and methanol) and two methods (soaking and boiling) were tried to select the suitable solvent and extraction method. After extraction, the best method was selected to continue the experiment. In the boiling method, 5 g of dried plants was rinsed again with distilled water and then boiled in 100 ml of 30% ethanol for 20 min. The same procedure was carried out with 30% methanol. For extraction by the soaking method, 2.5 g of the dried and washed plant was added to 50 ml of ethanol and placed on a stirrer for 24 h to obtain the extract. The same method was used to prepare the extract by methanol. In all of these methods, the obtained solutions were passed through filter paper and centrifuged at 9000 rpm for 15 min to separate the suspended particles and obtain the pure extracts. Fresh extracts were prepared for each experiment and stored in a refrigerator during the experiment.

2.4 Measurement of the Total Phenolic Content

To measure the total phenolic content, the method of Siddiqui et al. was used with a little modification [39]. For this purpose, 0.1 g of the extract was added to 10 ml of 50% ethanol and 100 μ l of this solution was added to 2.5 ml of 0.5 M Folin solution and 2 ml of 10% sodium carbonate solution. The mixture was kept in the dark for 1 h and then absorbance was read with a spectrophotometer at a wavelength of 760 nm. Standard Gallic acid solutions were prepared at 10, 40, 70, 100, 150, 300 and 400 ppm. The absorbance was plotted against concentration to obtain the calibration curve. The observed absorbance was converted to concentration using the linear equation obtained from the standard Gallic acid solutions. The total phenolic content was calculated as mg Gallic acid per gram extract using the following equation:

$$C = C1 \times V/m \quad (1)$$

where C is the total phenolic content as mg/g Gallic acid equivalents (GAE), C1 is Gallic acid concentration obtained from the standard curve, V volume of the extract in ml and m is the weight of the plant in g.

2.5 Synthesis of Silver Nanoparticles

A specific concentration of silver nitrate was first prepared and 20 ml of the extract was added to 60 ml of this silver nitrate solution in an Erlenmeyer flask. The Erlenmeyer flask was placed on a shaker at 220 rpm in the dark. The change of color to dark brown indicated that silver nanoparticles were formed. Samples were taken from the solution inside the Erlenmeyer flask at different times and studied the absorbance with a spectrophotometer at 300–700 nm. Presence of a peak in the range of 370–500 nm indicated synthesis of

silver nanoparticles. Different values of the variables such as time (30, 90 and 150 min), quantity of extract (5, 10, 20, 30 and 40 ml), reaction medium temperature (40, 60, 70 and 80 °C), pH of the solution (7, 8, 9, 10 and 11) and different concentrations of silver nitrate (0.001, 0.0025, 0.005, 0.01 and 0.05 M) were used to find the optimum conditions for silver nanoparticles synthesis. The obtained silver nanoparticles by *T. collinus* extract were separated from the solution by centrifuging at 15,000 rpm, then dispersed in distilled water and centrifuged again to get rid of any pollutant. This action repeated for three times and after the last one, the clean particles dried in oven at 60 °C.

2.6 Antibacterial Properties of the Extract

To study the biological properties of the extract, standard well agar diffusion method was carried out. For this aim, 100 μ l of *Staphylococcus aureus* (*S. aureus* PTCC 1112) and *Escherichia coli* (*E. coli* PTCC 1270) suspensions were prepared and poured into plates and cultured. A well was then made in each plate and filled with the extract and Erythromycin and Ampicillin disks were placed beside it for comparing the antibacterial activities. The plates were put in an incubator at 37 °C for 24 h and then the zones of inhibition were measured.

2.7 Study of the Antibacterial Properties of Silver Nanoparticles

The biological properties of the synthesis silver nanoparticles was studied using standard well agar diffusion method. At first different concentrations of silver nanoparticles (6000, 7000 and 8000 μ g/ml) were prepared. On the other hand, 100 μ l of *E. coli* and *S. aureus* bacteria was then poured into the prepared culture medium and uniformly spread using sterile cotton swab. Next, a pasture pipette was used to make 3 wells in each plate and the culture medium was removed from the wells. The wells were then filled with silver nanoparticles and the plates were placed in an incubator at 37 °C for 24 h. Finally, the zones of inhibition were measured.

3 Results and Discussion

3.1 Investigation of Total Phenolic Acid

Figure 1 shows the standard curve for Gallic acid in different concentration and Table 1 shows the amount of total phenolic compounds which calculated using Eq. 1. As it can be seen by using 30% Ethanol (v/v) as the extraction solvent and boiling the solution, extraction of phenolic compounds has the highest returns, so this method was used to continue the experiment.

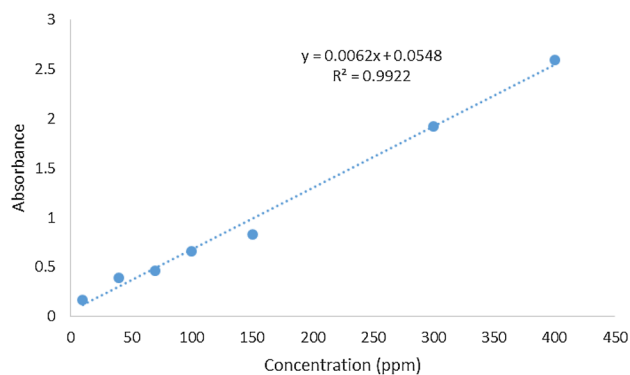


Fig. 1 Standard curve for Gallic Acid

Table 1 Phenolic content using different methods

Method/solvent	Total phenolic content (mg/g)
Ethanol/soaking	47.8
Ethanol/boiling	359
Methanol/soaking	160.7
Methanol/boiling	63.167

3.2 Initial Synthesis of the Silver Nanoparticles Using *Tragopogon collinus* Extract

After the addition of extract to the aqueous solution of silver nitrate, the color of the solution changed to dark brown, indicating successful synthesis of silver nanoparticles. Figure 2 shows the color of the solution before and after the synthesis of the nanoparticles. The spectra of the solution were acquired using a UV–Vis spectroscopy and the maximum absorbance was observed within the 300–700 nm range. It was noticed that the synthesized silver nanoparticles had their maximum absorbance at 400 nm. Since the extract and the silver nitrate solution were lack of absorbance at this wavelength, the observed absorption spectrum was only caused by the presence of silver nanoparticles.

3.3 Effect of Reaction Time on the Synthesis of Silver Nano Particles

Figure 3 shows the effect of the reaction time on the synthesis of the silver nano particles. As it can be seen, duration of synthesis also had a considerable effect on the synthesis and stability of nanoparticles [40].

Researchers studying about the synthesis of silver nanoparticles by using different plant species observed different optimum synthesis durations. This resulted from different laboratory conditions in the production of the nano particles [24]. The change in the color of the solution containing

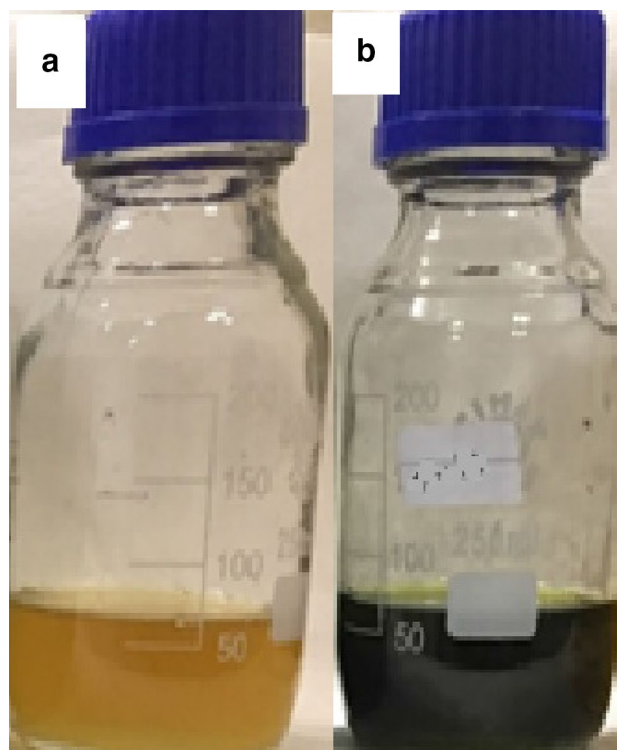


Fig. 2 Color change of the solution after 90 min. **a** The plant extract, **b** after synthesis of silver nanoparticles

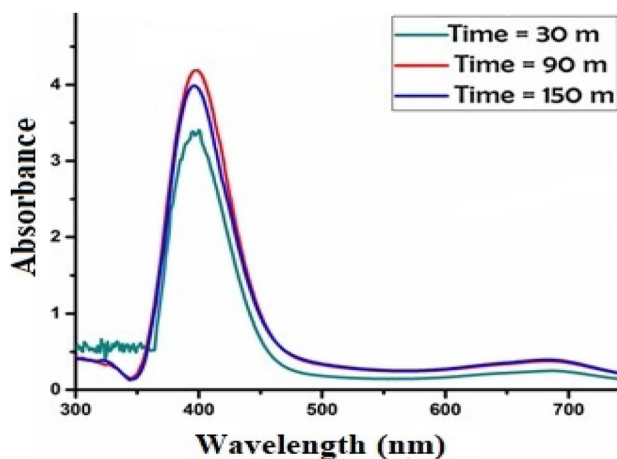


Fig. 3 Effect of the reaction time on the synthesis of silver nano particles

nanoparticles indicated changes in the surface resonance of the nanoparticles [41, 42]. If a solution containing nanoparticles maintains its color range for a long time, it indicates that the nanoparticles are uniformly dispersed and no agglomeration occurs [43]. In addition, absorption intensity is also an important criterion for the extent of nanoparticle formation so that higher absorption intensities indicate presence of more nanoparticles in the solution. As it can be seen

in Fig. 3 nanoparticle formation improved with increases in synthesis duration [25], but after 90 min the peak intensity declined due the agglomeration of nanoparticles due to their large size. Therefore, the optimum time for the synthesis of the nanoparticles was obtained to be 90 min. Furthermore the symmetry of the curve implied that the nanoparticles were synthesized homogeneously and had almost the same size.

3.4 Effects of pH on the Synthesis of Silver Nanoparticles

Reports indicate that the pH of the reaction medium considerably affects the shape and size of the nanoparticles. As pH is capable of altering the charge of macromolecules, it can affect their stability [22].

Figure 4 shows the effect of different pH on the synthesis of the particles. Absorption by the solution improved substantially with gradual increases in pH values. This resulted from the increase in the quantity of synthesized silver nanoparticles. A sharp and symmetric peak was observed at pH values of 9 and 10, whereas absorption declined at a pH of 11. This can be attributed to hydrolysis of silver ions causing production of stable types of hydroxide and preventing their entry into the bioreduction reaction. With increases in the pH value, the reduction reaction rate increased and hence the color change took place rapidly so that the color of the solution turned deep brown within a few minutes [23]. The shift in the maximum absorption peak indicated that the broadening of the absorption spectra at higher pH values resulted from the increase in the size of the silver nanoparticles [24, 44]. As the diameter of the nanoparticles increases, the energy required to excite the electrons at surface plasmon resonance decreases, consequently causing the absorption peak to shift toward longer wavelengths [22, 42]. In addition, at acidic pH values, nanoparticle growth stopped whereas

it improved at higher pH values, of course in some cases, for example synthesis of silver nano particles using banana peel extract, acidic pH was more suitable for the synthesis than alkali pH [21]. However, in this research, a pH of 11 caused the nanoparticles to experience an instability that could end up in their agglomeration if the pH remained at this value for a long time. This phenomenon was observed in other researches as well [22]. Compared to pH values of 7 and 8, the intensity of the peaks and hence the number of formed nanoparticles increased at pH values of 9, 10, 11 which was observed by using other types of plant extracts in previous works [24, 32, 41]. Therefore, compared to higher pH values, the maximum absorption reached the 396 nm wavelength at a pH of 10, indicating the synthesis of smaller and more homogeneous nanoparticles. Therefore, a pH of 10 was selected as the optimum pH value.

3.5 Amount of Extract Concentration on the Synthesis of Silver Nano Particles

To determine the optimum amount of the extract, 5, 10, 20, 30 and 40 ml of it was added to 50 ml AgNO_3 0.0025 M solutions and the pH of the solutions was adjusted to 10. After 90 min, the spectra were obtained from all the solutions using a UV–Vis spectrophotometer. As shown in Fig. 5, peak intensities increased by increasing in the amounts of the extract, which indicated an increase in the number of synthesized nanoparticles, because the number of functional groups reacting with the silver salt rose by using larger amounts of the extract [18]. Therefore, the number of synthesized nanoparticles increased, consequently improving the absorption intensity. In biosynthesis of nanoparticles using plants, the plants play the role of the agent that reduces metal ions and also stabilizes the synthesized nanoparticles [22]. Since *T. collinus* extract contains phenolic and flavonoid materials, these compounds play an important role in

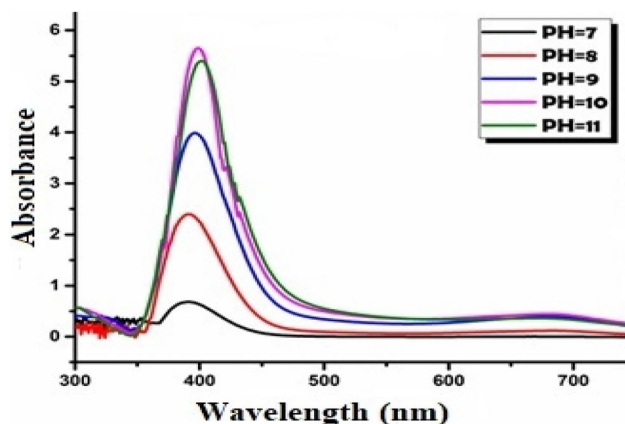


Fig. 4 Effect of pH on the synthesis of silver nano particles

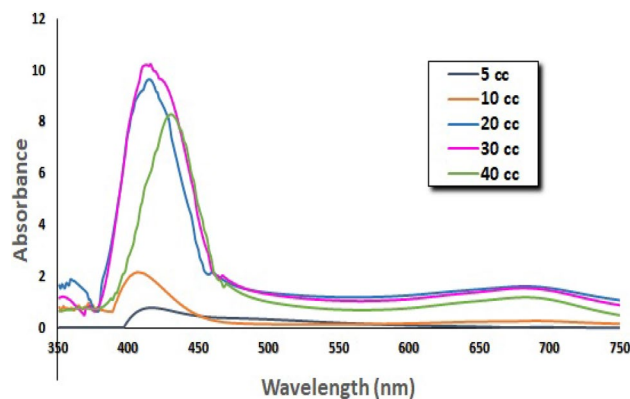


Fig. 5 Effect of the variable concentration of the extract on the synthesis of silver nano particles

the reduction of metal ions to metal atoms with nanometric dimensions and also in the stabilization of the synthetic nanoparticles.

Figure 5 indicates that the absorption by silver nanoparticles greatly increased when larger amounts of the extract were used. Increases in the quantity of the extract increased the quantity of secondary compounds in the solution as well as the synthesis of nanoparticles, following which absorption improved [25]. As it can be seen the absorbance was increased by increasing the quantity of the extract until it reaches to a volume of 40 ml of the extract and then decrease. At less than the optimum concentration of the extract, the metal ions are not completely reduced, giving rise to the production of lower amounts of nanoparticles. Considering the shift in λ_{max} towards shorter wavelengths, which indicated presence of smaller nanoparticles, addition of 20 ml of the extract led to the synthesis of finer nanoparticles as shown by the shift in the wavelength to 414 nm, so volume of 20 ml was chosen as the optimum quality.

3.6 Effect of Silver Nitrate Concentration on the Synthesis of Silver Nano Particles

To investigate the effect of silver nitrate on the synthesis of silver nanoparticles, silver nitrate concentrations of 0.001, 0.0025, 0.005, 0.01, 0.02 M were prepared and 20 ml of the extract was added to each one. After adjusting the pH of the solutions to pH 10, they were placed on a shaker for 90 min and their absorbance was read by UV–Visible spectrophotometry and the results showed in Fig. 6. As it can be seen, absorption improved with increases in the concentration of silver ions due to the increase in the amount of metal ions and hence the possibility of reduction of a larger number of silver ions [26, 32]. Consequently, more silver nanoparticles were synthesized and surface plasmon absorption intensity increased, leading to improved absorption. This increase in absorption continued up to the 0.0025 M concentration but

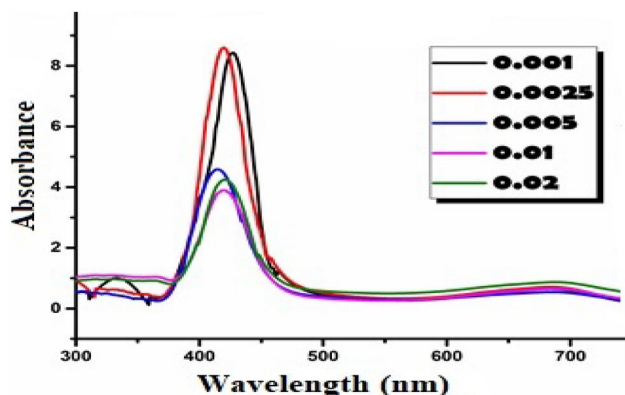


Fig. 6 Effect of silver nitrate concentration on the synthesis of silver nano particles

declined at higher concentrations due to the agglomeration of nanoparticles [27] and, hence, synthesis of larger nanoparticles. Therefore, the 0.0025 M concentration of silver nitrate solution increased absorption and also caused formation of finer nanoparticles by shifting λ_{max} to shorter wavelengths. Therefore, this concentration was selected as the optimum one.

3.7 Effect of the Temperature on the Synthesis of Silver Nano Particles

Another important factor in the synthesis of silver nanoparticles is temperature. Figure 7 shows the absorption spectrum of silver nanoparticles at 40, 60, 70, and 80 °C. It is expected that at higher temperatures, silver nitrate reduction took place more rapidly and the color change happened faster [22], but increases in temperature from 40 to 80 °C did not considerably affect the synthesis of silver nanoparticles. Moreover, temperatures from 60 to 80 °C did not cause any tangible increase in peak intensity to indicate an increase in the number of synthesized nanoparticles. The lack of increase in absorption intensity under these conditions indicated that there was no change in the size or shape of the nanoparticles. Considering the increase in peak intensity at 40 °C, this temperature was selected as the optimum value, this result is against with the result obtained by [21, 24].

3.8 FT-IR Analysis of the Synthesized Silver Nano Particles

FT-IR spectra of the synthesis silver nanoparticles was obtained and the result shows in Fig. 8. The peak at 3385 cm^{-1} , was attributed to the OH stretching vibration of hydroxyl group which shows the presence of phenolic and alcoholic compounds in the extract. The peak at 2921 cm^{-1} is associated with the NH stretching vibration

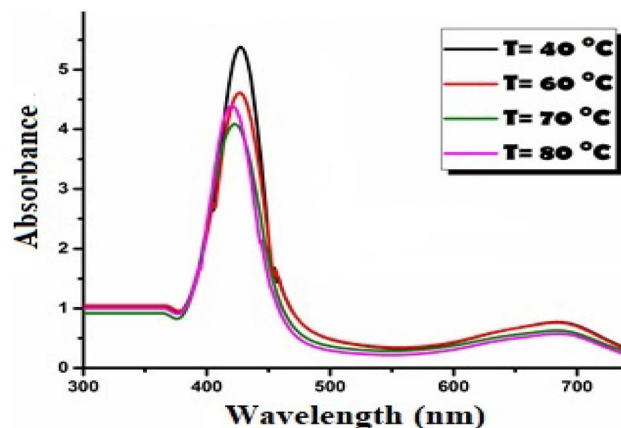
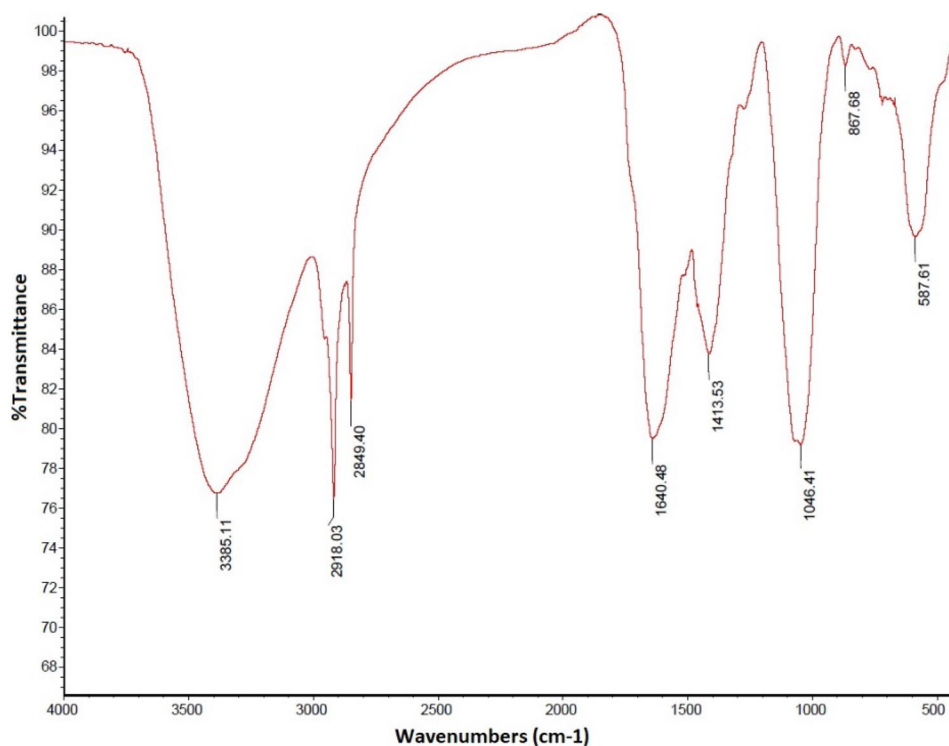


Fig. 7 Effect of temperature on the synthesis of silver nano particles

Fig. 8 FT-IR spectra of synthesized silver nano particles



of amine groups in the extract. The characteristic peak was observed at 1640 cm^{-1} due to the C–O stretching vibration of amide I and the one at 1413 cm^{-1} associated with bending vibrations of NH_2 group in amide II. Since the CO group in the amino acids tends to attach to the nanoparticles, this peak indicates that the silver nanoparticles are bonded to the proteins present in the extract. Also, the absorption band at 1046 cm^{-1} is related to the stretching vibrations of the C–C group in sugar and fat. The presence of these functional groups indicates that the extract exhibits both specific regeneration and stabilizing properties, thus preventing the particles from adhering and agglomerating [45, 46]

3.9 Identification of Silver Nanoparticles Using X-ray Diffraction Patterns

Figure 9 shows the XRD patterns of the synthesized silver nano particles. Considering the positions of the peaks occurring within the 2θ angles of 38.67° , 44.01° , 64.67° and 76.4° that correspond to the cubic crystallographic planes (311), (220), (200) and (111), respectively, it was proved that silver nanoparticles were synthesized. Presence of sharp peaks indicated a high degree of crystallinity. Since impurity peaks were not observed, the synthesized nanoparticles were of high purity. Use of the Debye–Scherrer equation showed that the size of the silver nanoparticles was about 7 nm.

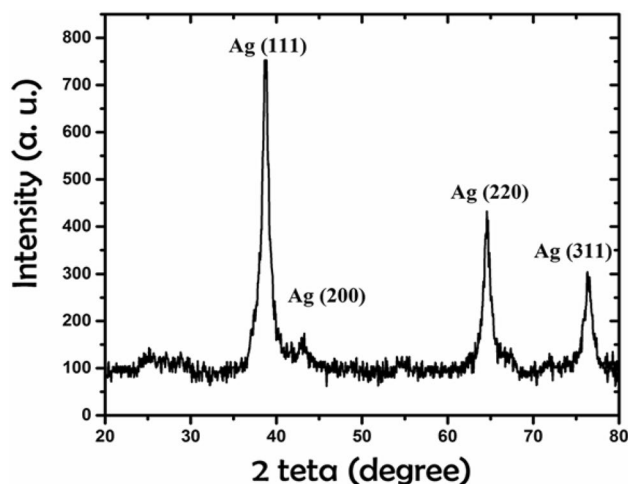


Fig. 9 XRD patterns of the synthesized silver nano particles

3.10 TEM Images of Silver Nanoparticles

Figure 10 shows TEM images of the synthesized nanoparticles. According to the TEM images, the silver nanoparticles were spherical and ranged in size from 7 to 18 nm. The particles were well dispersed and no particle adhesion or agglomeration was observed. The small size of the particles was due to selection of suitable reaction condition and the different size of the synthesized nanoparticles might be due to the presence of more than one reducing agent in the plant [6].

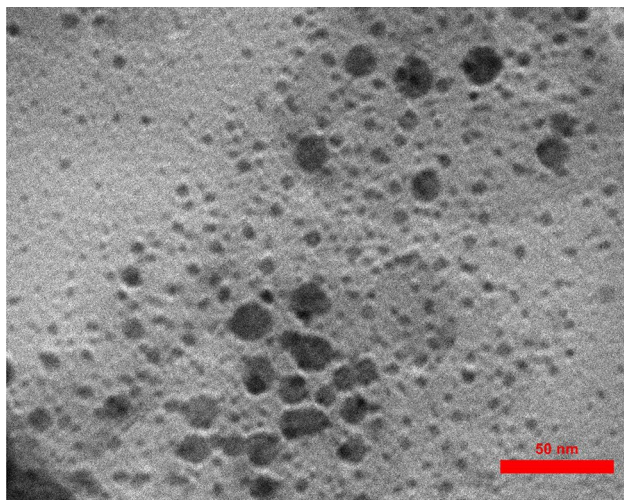


Fig. 10 TEM images of the synthesized silver nano particles

Table 2 The size of the green synthesized silver nano particles

Plant extract	Size (nm)	References
<i>Givotia moluccana</i>	30–40	[9]
<i>Artemisia vulgaris</i>	25	[10]
<i>Cinnamomum tsoi</i>	10	[18]
<i>Melissa officinalis</i>	12	[11]
<i>carob</i>	40	[23]
<i>olive</i>	15–30	[24]
<i>Datura stramonium</i>	15–20	[27]
<i>Combretum erythrophyllum</i>	13.62	[28]
<i>Shikakai</i>	20–40	[40]
<i>Sida cordifolia</i>	3–6	[30]

Table 2 shows the size range of the synthesized silver nano particles using green method by the researchers. Synthesis of silver nano particles using *T. collinus* extract producing fine nano particles in the range that many researchers have reported.

3.11 Study of Biological Properties of the Synthesized Silver Nano Particles

Images related to antibacterial properties and zones of inhibition in the presence of *T. collinus* extract alone, AgNO_3 solution and synthesized silver nanoparticles by *T. collinus* plant extract at concentrations of 6000, 7000 and 8000 $\mu\text{g/ml}$ in the vicinity of *S. aureus* and *E. coli* are presented in Fig. 11. The diameter of inhibition zone was reported in Table 3 as well. As shown in Fig. 10 while the Ampicillin disk (IPM in the picture a and b) shows a relatively large inhibition zone for both types of the bacteria, the *T. collinus* extract has no antibacterial effect. Furthermore silver nitrate

solution has no antibacterial properties in both of the culture moieties as well. It can be inferred from Table 3 that the synthesized nanoparticles exhibited antibacterial properties for both Gram positive and Gram negative types of bacteria and the diameter of the zone of inhibition was larger at a nanoparticle concentration of 8000 $\mu\text{g/ml}$. The diameter of the zone of inhibition was the largest and the antibacterial property of the nanoparticles is the highest in the presence of *S. aureus*. Better performance of synthesized silver nano particles to prevent *S. aureus* bacteria growth is in good agreement with previous reports [9, 10, 14, 24–26, 28, 47]. On the other hand several papers reported that zones of inhibition for *E. coli* was larger than *S. aureus* using silver nano particles [11, 21, 23, 27, 48].

Nanoparticles obtained by chemical methods cause drug toxicity and environmental problems. These risks can be mitigated by green synthesis and through application of plant extracts as reducing agents. The results of antibacterial activity of the synthesized silver nanoparticles on the studied bacteria and comparison of their antibacterial activities with those of antibiotics indicated that these nanoparticles had more antibacterial activity against Gram-positive bacteria than against Gram-negative bacteria.

Since these nanoparticles make the plasma membrane unstable, they reduce the levels of adenosine triphosphate (ATP) in the cells. This action targets bacterial cell membranes and kills the bacteria. Silver nanoparticles disrupt the inhibitory components present in the outer membranes of the bacteria and cause exponential release of molecules such as lipopolysaccharides (LPSs) and purines outside of the cytoplasmic membranes. Not only do silver nanoparticles adhere to the surface of bacterial cell membranes but also penetrate into the bacterial cells, inactivate their enzymes and kill the bacteria by producing hydrogen peroxide. Therefore, these factors are the reasons for inhibition of bacterial growth by silver nanoparticles [2, 16, 49].

It has been suggested that when in a free state, DNA molecules can replicate efficiently, while they lose their ability to replicate when they are in a concentrated state. Therefore, when silver ions penetrate into the microbial cell, the DNA molecules change into the concentrated state and lose their ability to replicate, which results in the death of the cell. It has also been reported that heavy metals react with proteins by binding to thiol groups and inactivate them. Silver is inherently an antimicrobial and antibacterial substance, but silver nanoparticles exhibit effective antimicrobial properties compared to other salts due to their substantial high surface area, which allows better contact with microorganisms [16, 49].

In this research, silver nanoparticles were synthesized using a green biosynthesis method applied to the *T. collinus* extract, a native plant in Iran with therapeutic properties. Nanoparticles synthesis by plants extract can be used for

Fig. 11 Antibacterial properties and zones of inhibition in the presence of extract (**a**, **b**), AgNO₃ solution (**c**, **d**) and synthesized silver nanoparticles (**e**, **f**) at concentrations of 6000, 7000 and 8000 µg/ml in the vicinity of *S. aureus* (**a**, **c**, **e**) and *E. coli* (**b**, **d**, **f**)

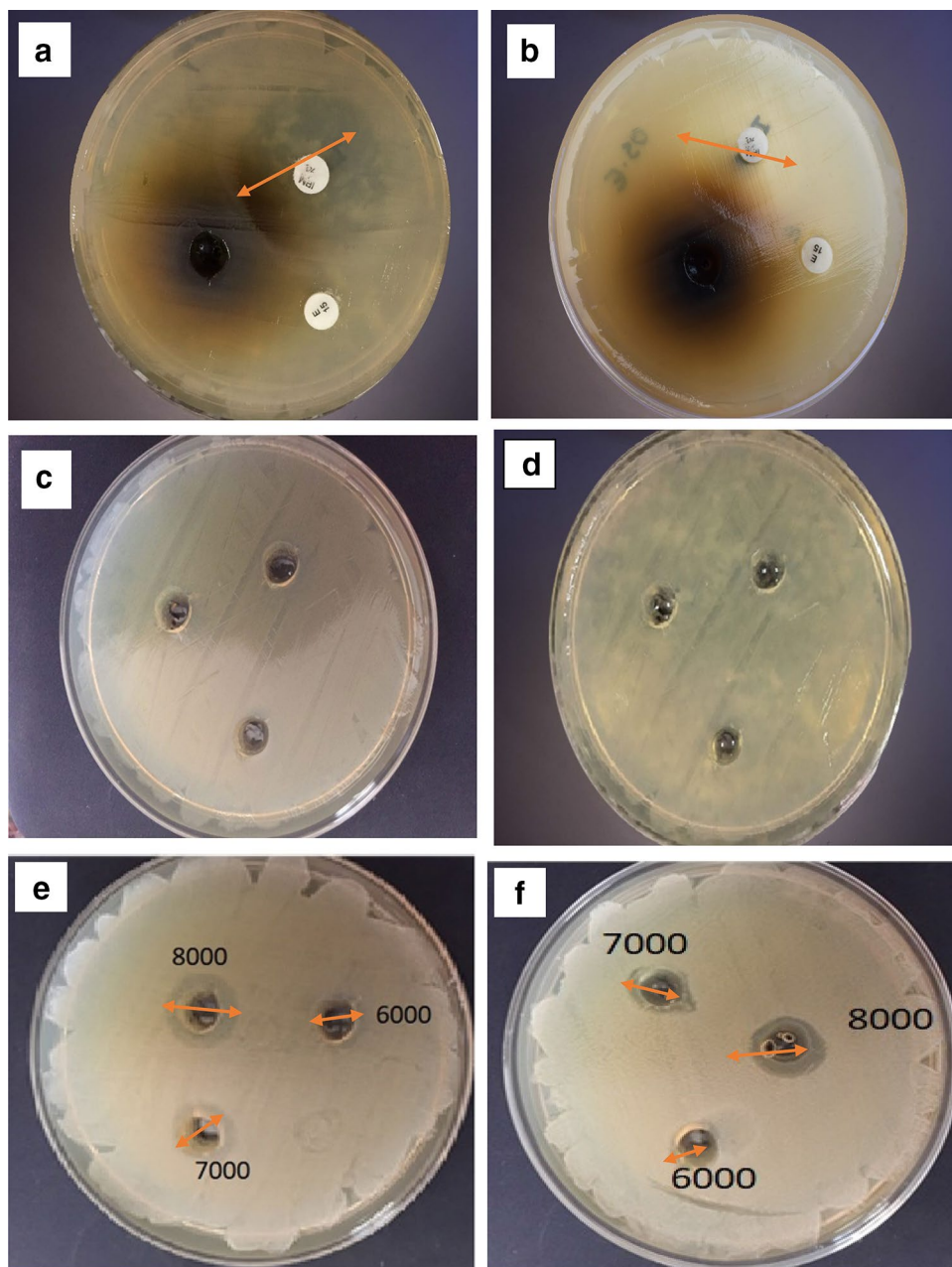


Table 3 Zones of inhibition in the presence of synthesized silver nanoparticles at different concentration

Bacteria type	Concentration (µg/ml)	Inhibition zone (mm)
<i>S. aureus</i>	6000	2
	7000	5
	8000	10
<i>E. coli</i>	6000	4
	7000	7
	8000	8

various applications such as drug delivery. Advantages of these methods include their simplicity and low cost as well as the possibility of producing nanoparticles with different shapes and identical sizes. The range of changes in the nanoparticle size can be solved by various methods such as changes in pH and in extract volume and use of different salt solution concentrations and reaction duration to obtain optimal conditions. In this study, the optimum conditions for the synthesis of silver nanoparticles were temperature of 40 °C, extract volume of 20 ml, silver nitrate concentration of 0.0025 M and pH 10. Ultraviolet–visible spectrophotometric analysis confirmed the presence of silver nanoparticles. TEM images and X-ray diffraction analysis showed that

the prepared nanoparticles were spherical and their average size was 7–18 nm. Moreover, the presence of OH, NH, and CO functional groups in the FT-IR spectrum indicated the reducing power and the stabilizing property of the extract. The compounds in the extract attached to the nanoparticles and prevented agglomeration of the nanoparticles and their adhesion to each other.

Results of the antibacterial properties indicated that the synthetic nanoparticles had antibacterial nature against both Gram-positive and Gram-negative bacteria, but they were more active against the gram-positive *S. aureus* and the inhibiting bacterial growth was achieved at a concentration of 8000 µg/ml of the prepared silver nano particles. Since chemicals were not used in this synthesis, the prepared nanoparticles can be used as an antibacterial substitute for antibiotics.

Compliance with Ethical Standards



Conflict of interest No potential conflict of interest was reported by the authors.

References

- P. Gajjar, B. Pettee, D.W. Britt, W. Huang, W.P. Johnson, A.J. Anderson, *J. Biol. Eng.* **3**, 9 (2009)
- B. Thomas, A. Arul Prasad, S. Mary Vithiya, *J. Nanostruct.* **8**, 179 (2018)
- M. Zargar, A.A. Hamid, F.A. Bakar, M.N. Shamsudin, K. Shameli, F. Jahanshiri, F. Farahani, *Molecules* **16**, 6667 (2011)
- M. Zia, S. Gul, J. Akhtar, I.U. Haq, B.H. Abbasi, A. Hussain, S. Naz, M.F. Chaudhary, *IET Nanobiotechnol.* **11**, 193 (2017)
- Hitesh, S. Lata, *Mater. Today* **5**, 6227 (2018)
- M.P. Patil, R.D. Singh, P.B. Koli, K.T. Patil, B.S. Jagdale, A.R. Tipare, G.-D. Kim, *Microb. Pathog.* **121**, 184 (2018)
- K.N. Thakkar, S.S. Mhatre, R.Y. Parikh, *Nanomedicine* **6**, 257 (2010)
- H.Y. El Kassas, A.A. Attia, *Asian Pac. J. Cancer Prev.* **15**, 1299 (2014)
- S.S. Sana, L.K. Dogiparthi, *Mater. Lett.* **226**, 47 (2018)
- T. Rasheed, M. Bilal, H.M.N. Iqbal, C. Li, *Colloids Surf. B* **158**, 408 (2017)
- Á. de Jesús Ruíz-Baltazar, S. Y. Reyes-López, D. Larrañaga, M. Estévez, R. Pérez, *Results Phys.* **7**, 2639 (2017)
- C. Rice-evans, *Free Radic. Biol. Med.* **36**, 827 (2004)
- S. Gurunathan, J.W. Han, D.-N. Kwon, J.-H. Kim, *Nanoscale Res. Lett.* **9**, 373 (2014)
- S. Ahmed, K. Saifullah, M. Ahmad, B.L. Swami, S. Ikram, *J. Radiat. Res. Appl. Sci.* **9**, 1 (2016)
- M. Moghtader, H. Salari, H. Mozafari, A. Farahmand, *J. Mol. Cell. Res.* **29**, 331 (2016)
- J.R. Morones, J.L. Elechiguerra, A. Camacho, K. Holt, J.B. Kouri, J.T. Ramírez, M.J. Yacaman, *Nanotechnology* **16**, 2346 (2005)
- S. Dinesh, S. Karthikeyan, P. Arumugam, *Arch. Appl. Sci. Res.* **4**, 178 (2012)
- S. Babu Maddinedi, B. K. Mandal, S. K. Maddili, *J. Photochem. Photobiol. B* **167**, 236 (2017)
- O. Choi, K.K. Deng, N.-J. Kim, L. Ross, R.Y. Surampalli, Z. Hu, *Water Res.* **42**, 3066 (2008)
- K.A. Willets, R.P. Van Duyne, *Annu. Rev. Phys. Chem.* **58**, 267 (2007)
- H.M.M. Ibrahim, *J. Radiat. Res. Appl. Sci.* **8**, 265 (2015)
- A. Verma, M.S. Mehata, *J. Radiat. Res. Appl. Sci.* **9**, 109 (2016)
- A.M. Awwad, N.M. Salem, A.O. Abdeen, *Int. J. Ind. Chem.* **4**, 29 (2013)
- M.M.H. Khalil, E.H. Ismail, K.Z. El-Baghdady, D. Mohamed, *Arab. J. Chem.* **7**, 1131 (2014)
- P. Logeswari, S. Silambarasan, J. Abraham, *J. Saudi Chem. Soc.* **19**, 311 (2015)
- K. Jyoti, M. Baunthiyal, A. Singh, *J. Radiat. Res. Appl. Sci.* **9**, 217 (2016)
- M. Gomathi, P.V. Rajkumar, A. Prakasam, K. Ravichandran, *Resour. Eff. Technol.* **3**, 280 (2017)
- O.T. Jemilugba, E.H.M. Sakho, S. Parani, V. Mavumengwana, O.S. Oluwafemi, *Colloid Interface Sci. Commun.* **31**, 100191 (2019)
- U. Kumar Sur, B. Ankamwar, S. Karmakar, A. Halder, P. Das, *Mater. Today* **5**, 2321 (2018)
- P.N.V.K. Pallela, S. Ummey, L.K. Ruddaraju, S.V.N. Pammi, S.-G. Yoon, *Microb. Pathog.* **124**, 63 (2018)
- N. Khorasani, J. Baharara, A. Iranbakhsh, T. Ramezani, *KAUMS J. (FEYZ)* **19**, 457 (2016)
- F. Eya'ane Meva, M. L. Segnou, C. Okalla Ebongue, A. A. Ntomba, P. Belle Ebanda Kedi, V. Deli, M.-A. Etoh, E. Mpondo Mpondo, *Rev. Bras. Farmacogn.* **26**, 640 (2016)
- M. Dhayalan, M.I.J. Denison, A.J. L. K. Krishnan, N.G. N. Nat. *Prod. Res.* **31**, 465 (2017)
- S. Raj, S. Chand Mali, R. Trivedi, *Biochem. Biophys. Res. Commun.* **503**, 2814 (2018)
- D. Hebbalalu, J. Lalley, M.N. Nadagouda, R.S. Varma, A.C.S. Sustain, *Chem. Eng.* **1**, 703 (2013)
- S. Priyadarshini, S. Sulava, R. Bhol, S. Jena, *Curr. Sci.* **117**, 8 (2019)
- I. Torres, J. Bustamante, D. A. Sierra (ed.), *VII Latin American Congress on Biomedical Engineering CLAIB 2016, Bucaramanga, Santander, Colombia, October 26th-28th, 2016* (Springer, Singapore, 2017)
- M.N. Nadagouda, R.S. Varma, *Green Chem.* **10**, 859 (2008)
- N. Siddiqui, A. Rauf, A. Latif, Z. Mahmood, *J. Taibah Univ. Med. Sci.* **12**, 360 (2017)
- K.P. Kumar, W. Paul, C.P. Sharma, *Process Biochem.* **46**, 2007 (2011)
- C. Noguez, *J. Phys. Chem. C* **111**, 3806 (2007)
- V. Amendola, O.M. Bakr, F. Stellacci, *Plasmonics* **5**, 85 (2010)
- N. Ahmad, S. Sharma, MdK Alam, V.N. Singh, S.F. Shamsi, B.R. Mehta, A. Fatma, *Colloid Surf. B* **81**, 81 (2010)
- Y. Qin, X. Ji, J. Jing, H. Liu, H. Wu, W. Yang, *Colloid Surf. A* **372**, 172 (2010)
- D. Nayak, S. Ashe, P.R. Rauta, M. Kumari, B. Nayak, *Mater. Sci. Eng. C* **58**, 44 (2016)
- S. Raja, V. Ramesh, V. Thivaharan, *Arab. J. Chem.* **10**, 253 (2017)
- P. Thatoi, R.G. Kerry, S. Gouda, G. Das, K. Pramanik, H. Thatoi, J.K. Patra, *J. Photochem. Photobiol. B* **163**, 311 (2016)
- K. Roy, C.K. Sarkar, C.K. Ghosh, *Appl. Nanosci.* **5**, 945 (2015)
- E.T. Hwang, J.H. Lee, Y.J. Chae, Y.S. Kim, B.C. Kim, B.-I. Sang, M.B. Gu, *Small* **4**, 746 (2008)

Publisher's Note Springer Nature remains neutral with regard to jurisdictional claims in published maps and institutional affiliations.

Affiliations

Roya Seifipour¹  · Maryam Nozari²  · Leila Pishkar¹ 

✉ Maryam Nozari
m_nozari@iau-tnb.ac.ir

² Faculty of Chemistry, Islamic Azad University, Tehran North Branch, Tehran, Iran

¹ Department of Biology, Islamshahr Branch, Islamic Azad University, Islamshahr, Iran